Supplemental Figure 1

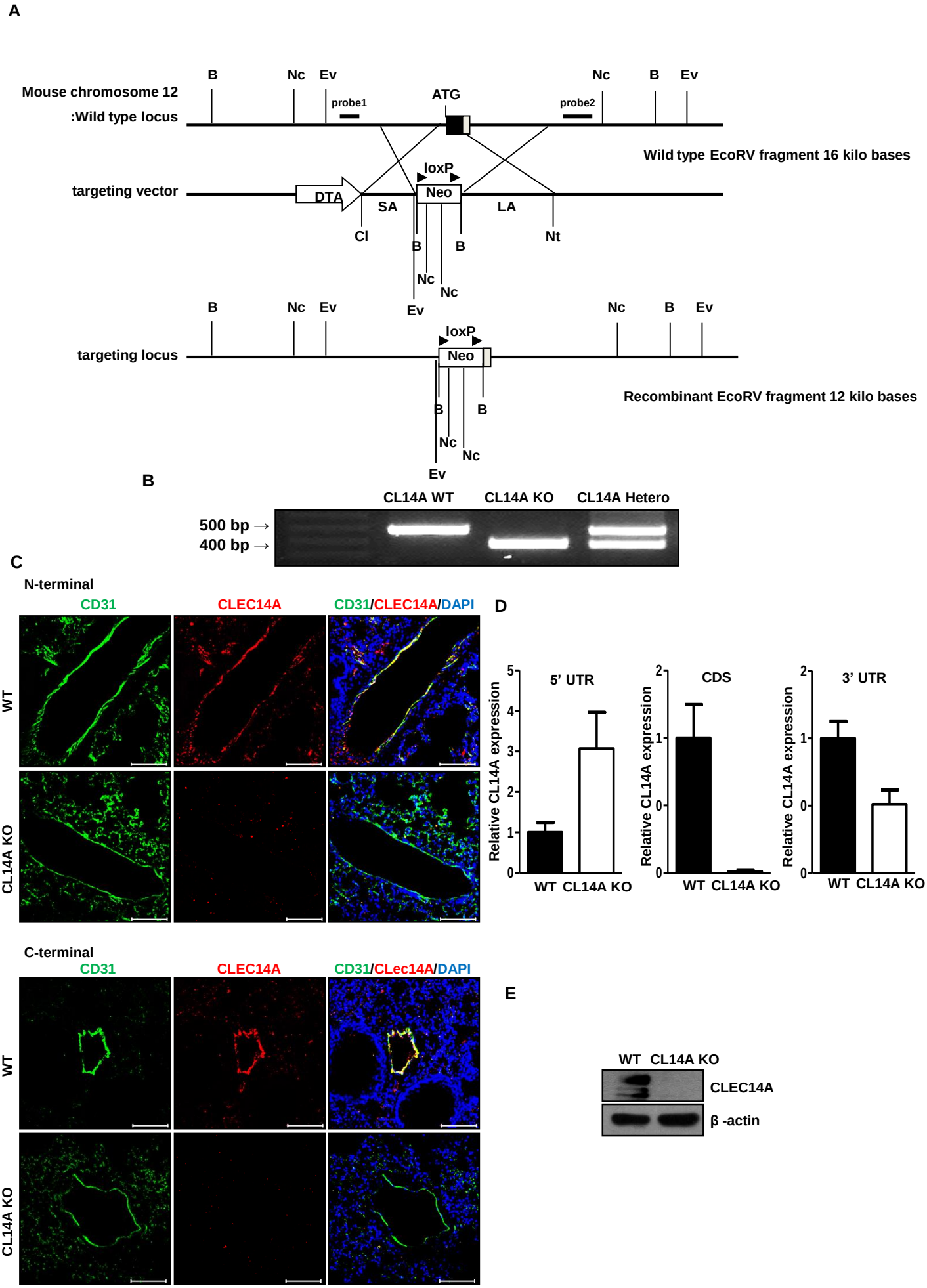

Supplemental Figure 1

Generation of CLEC14A KO mice

(**A**) Schematic diagram of the targeting strategy used to generate the CLEC14A KO mouse. (**B**) Genotyping PCR to confirm CLEC14A KO. A band near 500 bp represents the WT CLEC14A allele, a band near 400 bp represents the CLEC14A KO allele and 2 bands at 500 bp and 400 bp represent heterozygous mice. (**C**) Flat-mount staining of WT and CLEC14A mouse lung sections for CD31 and CLEC14A with two different antibodies, (CLEC14A with N-terminal and C-terminal antibodies). n = 3 per group. Scale bar: 100 μm. (**D**) Relative mGAPDH-normalised real time-PCR analysis of cDNA generated from WT and CLEC14A mice lung lysates for the 5'-UTR, CDS and 3'-UTR of *clec14a*. (**E**) Western blot analysis of CLEC14A protein expression from WT and CLEC14A KO mice lung lysates. n = 6 per group. *, $P < 0.05$; **, $P < 0.005$; ***, $P < 0.0001$ by paired, 2-tailed Student's *t* test. Error bars represent the mean $\pm$ SD.

Supplemental Figure 2

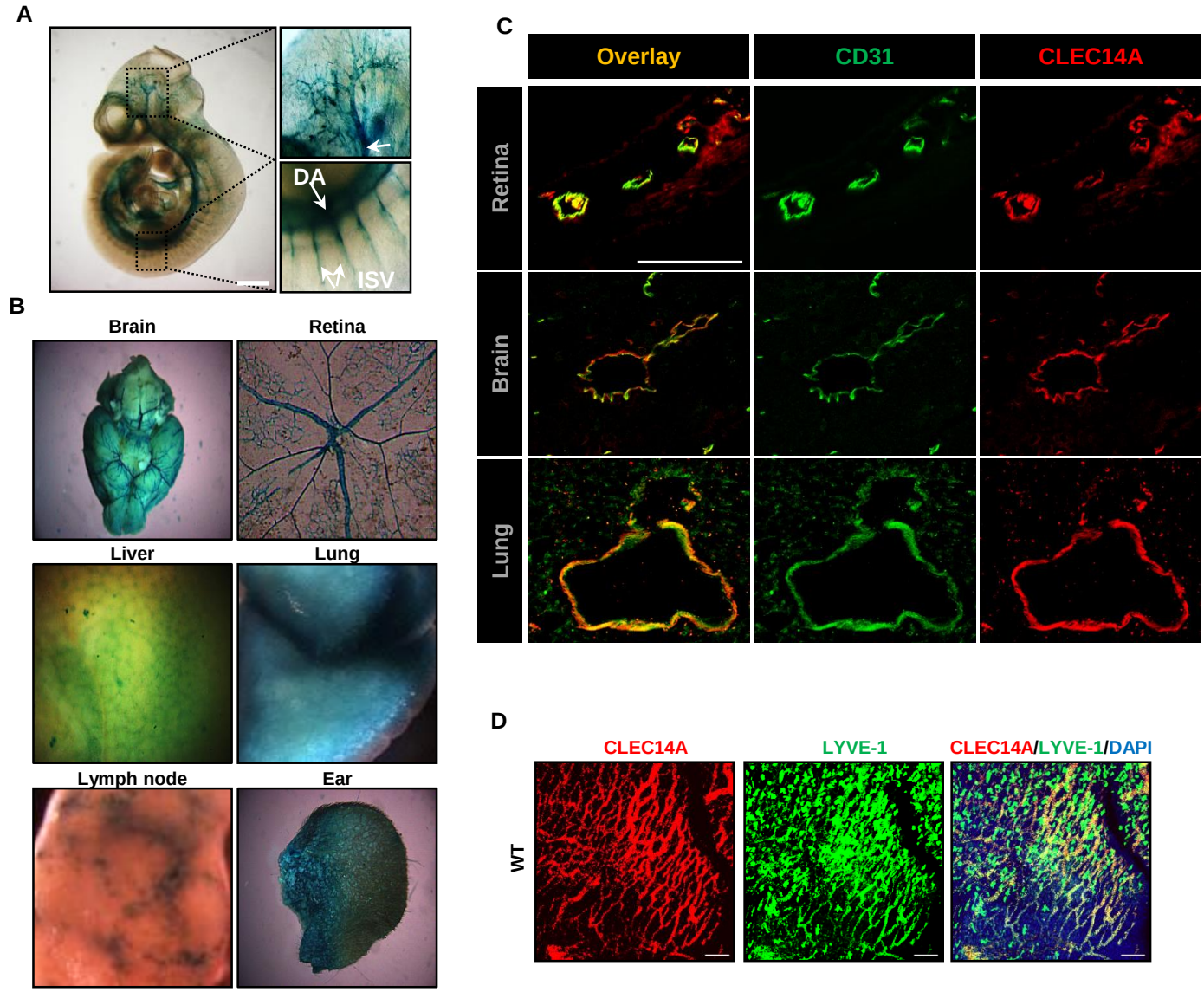

Supplemental Figure 2

Blood and lymphatic EC specific expression of CLEC14A

(**A**) LacZ staining of CLEC14A KO mice at E10.5. ICA, internal carotid artery; DA, dorsal aorta; ISV, intersomitic vessels. n = 3 per group. Scale bar: 50 μm. (**B**) LacZ staining of adult CLEC14A KO mouse brain, retina, liver, lymph nodes, lungs and ears. (**C**) Immunostaining of 5-week-old WT mouse retina, brain and lungs. Scale bar: 100 μm (**D**) Immunostaining of E15.5 WT forelimb for CLEC14A and LYVE-1. Scale bar: 100 μm. All experiments were repeated on at least 3 different sets of WT and KO littermates.

Supplemental Figure 3

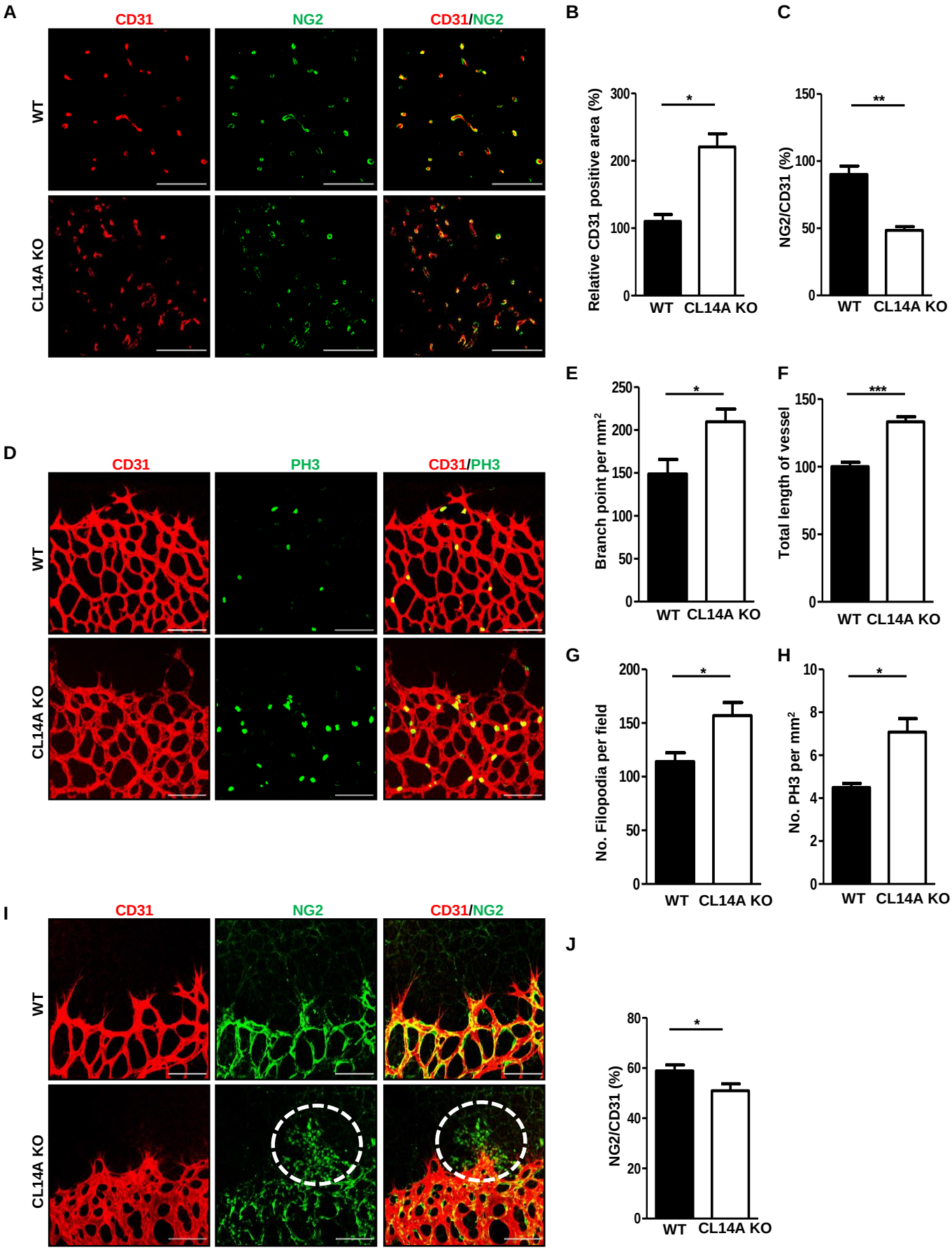

Supplemental Figure 3

CLEC14A deletion increases blood vessel density and reduces pericyte coverage

(**A**-**C**) Immunostaining and quantification of blood vessels and pericytes (blood vessels, CD31-positive in red; pericytes, NG2-positive in green) in sagittal sections of E13.5 brain from WT and CLEC14A KO mice. n = 6 per group. (**D**) Whole-mount preparations of P5 retinas from WT and CLEC14A KO pups immunostained for CD31 and the proliferation marker PH3. n = 6 per group. (**E**-**H**) Quantification of the number of branch points, total length of vessels, number of filopodia and number of PH3 puncta. n = 6 per group. (**I** and **J**) Whole-mount preparations of P5 retinas from WT and CLEC14A KO pups immunostained with CD31 and NG2 antibodies. Quantification of pericyte coverage per blood vessel (blood vessels, red; pericytes, green). n = 6 per group. Scale bar: 100 μm. All experiments were repeated on at least 6 different sets of WT and KO littermates. *, $P < 0.05$; **, $P < 0.005$; ***, $P < 0.0001$ by paired, 2-tailed Student's *t* test. Error bars represent the mean $\pm$ SD.

Supplemental Figure 4

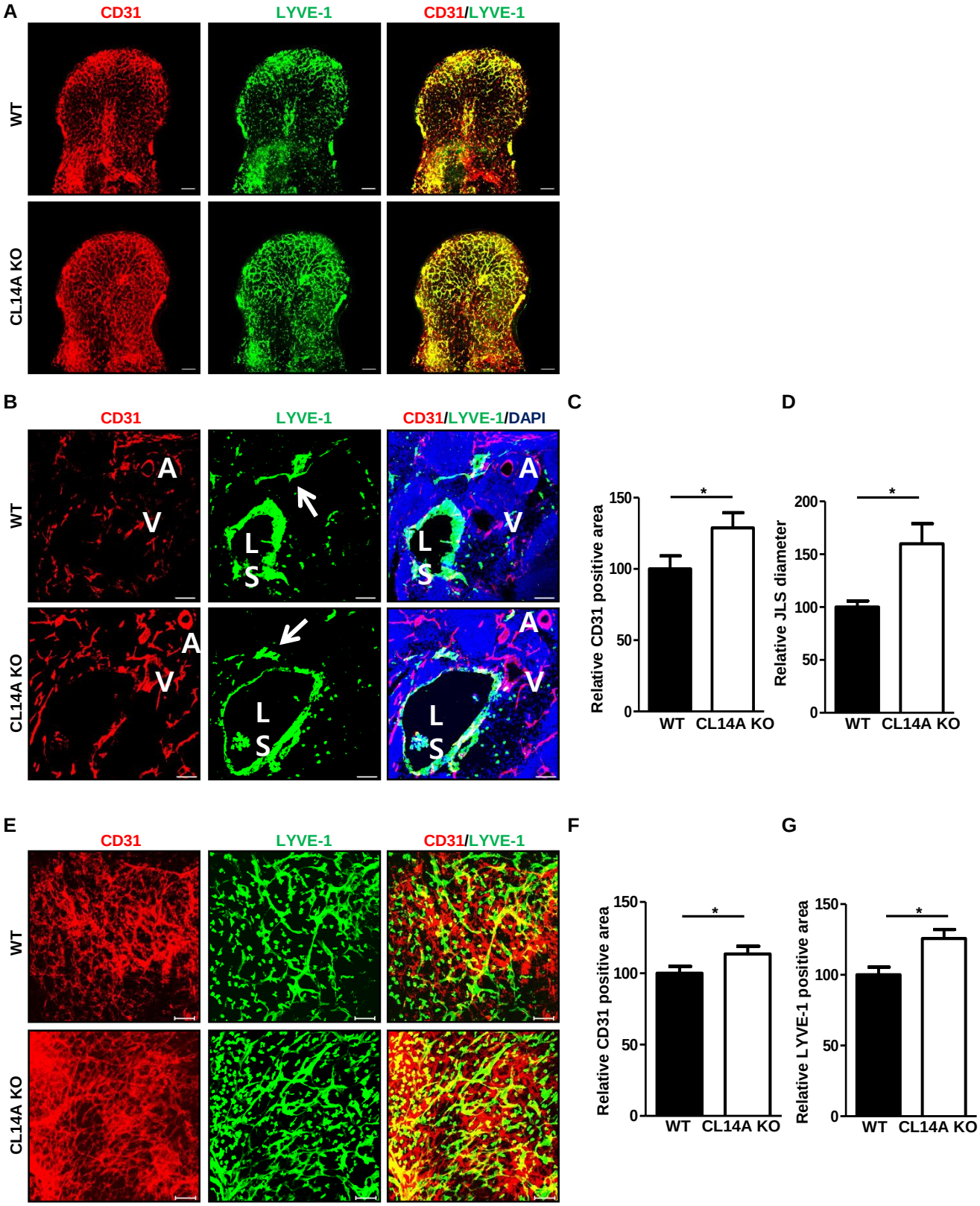

Supplemental Figure 4

Loss of CLEC14A increases blood and lymphatic vessel density and causes jugular lymph sac dilation

(**A**) Whole-mount staining of E11.5 WT and CLEC14A KO embryo forelimbs with CD31 and LYVE-1 antibodies demonstrating increased blood and lymphatic vessel density. n = 3 per group. (**B**) Transverse sections of E13.5 WT and CLEC14A KO embryos immunostained for CD31 and LYVE-1 demonstrating increased blood vessel density and jugular lymph sac diameter. n = 3 per group. Scale bar: 100 μm. (**C** and **D**) Quantification of relative blood vessel density and jugular lymph sac diameter (% of control). Scale bar: 100 μm. (**E**) Flat-mount staining of E13.5 WT and CLEC14A KO embryo forelimbs for CD31 and LYVE-1 demonstrating increased blood lymphatic vessel density. n = 3 per group. Scale bar: 100 μm. (**F** and **G**) Quantification of relative blood vessel density and lymphatic vessel density (% of control). All experiments were repeated on at least 3 different sets of WT and KO littermates. *, $P < 0.05$; **, $P < 0.005$; ***, $P < 0.0001$ by paired, 2-tailed Student's *t* test. Error bars represent the mean $\pm$ SD.

Supplemental Figure 5

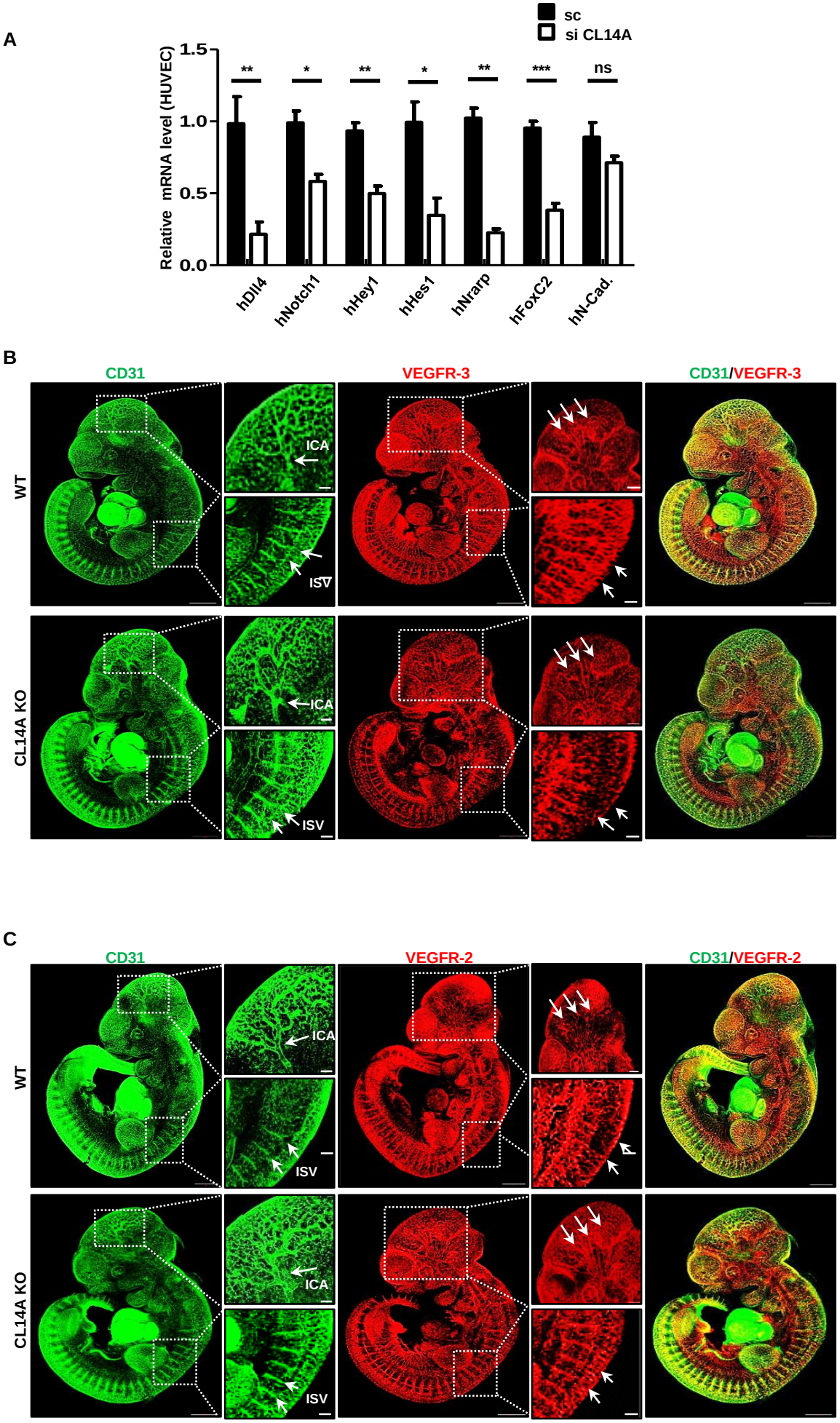

Supplemental Figure 5

CLEC14A deficiency alters the expression levels of Notch/Dll4 and downstream Notch target genes in HUVECs, and attenuates VEGFR-3 expression and promotes VEGFR-2 expression in E10.5 CLEC14A KO embryos

(**A**) Relative GAPDH-normalised mRNA levels of Notch/Dll4 and Notch target genes in HUVECs following knockdown of CLEC14A. (**B**) Whole-mount staining of E10.5 WT and CLEC14A KO embryos with CD31 and VEGFR-3, demonstrating lower VEGFR-3 expression in the ICA and ISV (arrows) of KOs. n = 3 per group. (**C**) Whole-mount staining of E10.5 WT and CLEC14A KO embryos with CD31 and VEGFR-2, demonstrating higher VEGFR-2 expression in the ICA and ISA (arrows) of KOs. n = 3 per group. ICA, internal carotid artery; ISV, intersomitic vessels. Scale bar: 100 μm. All experiments were repeated on at least 3 different sets of WT and KO littermates. Error bars represent the mean $\pm$ SD.

Supplemental Figure 6

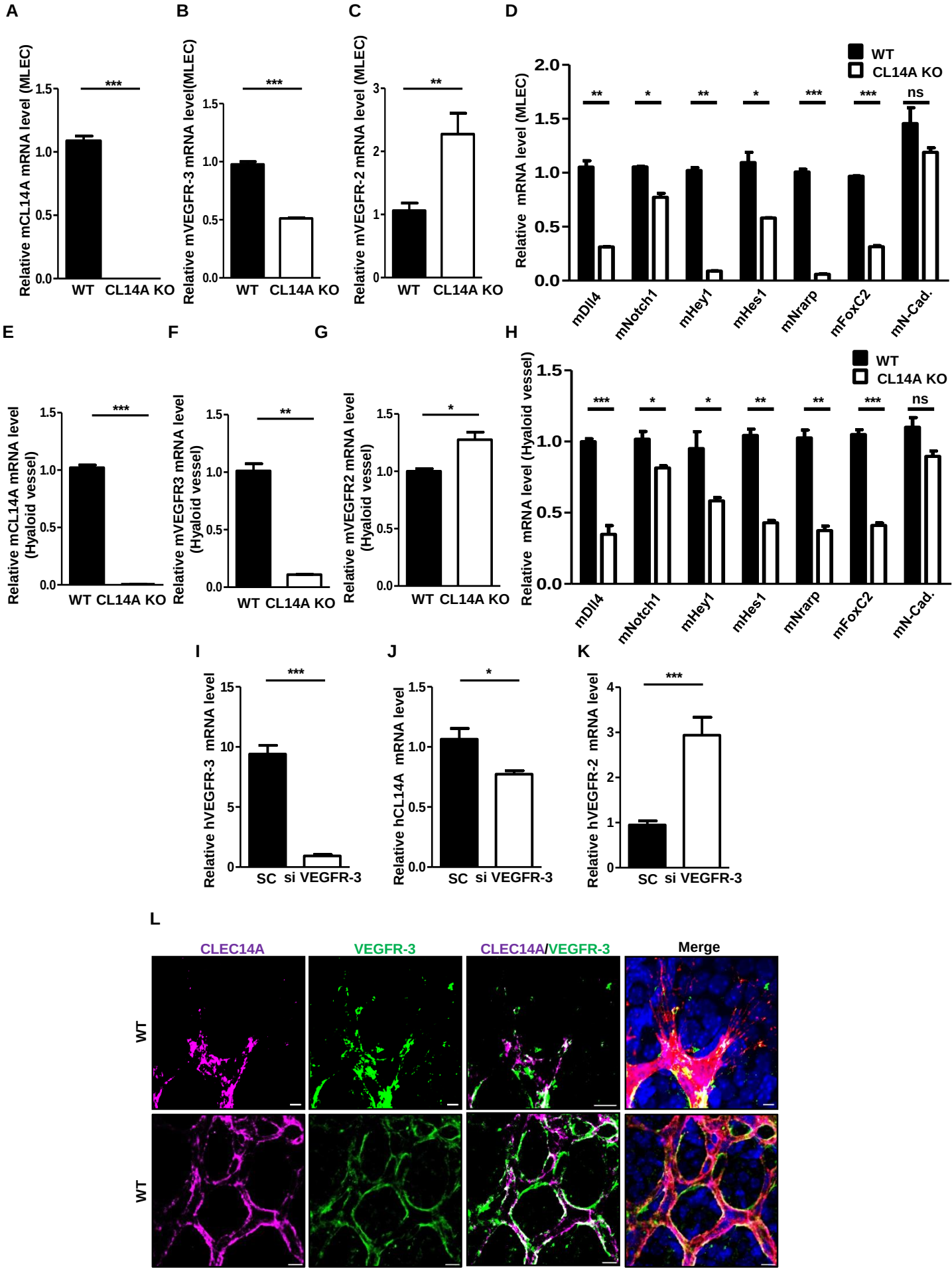

Supplemental Figure 6

CLEC14A deficiency alters the expression levels of VEGFR-3, VEGFR-2, Notch/Dll4 and downstream Notch target genes in murine lung EC and hyaloid vessels, and silencing of VEGFR-3 alters the expression levels of CLEC14A and VEGFR-2.

(**A**-**D**) Relative GAPDH-normalised mRNA levels of CLEC14A, VEGFR-3, VEGFR-2, Notch/Dll4 and Notch target genes in murine lung ECs (MLECs) from WT and CLEC14A KO mice. n = 3 per group. (**E**-**H**) Relative GAPDH-normalised mRNA levels of CLEC14A, VEGFR-3, VEGFR-2, Notch/Dll4 and Notch target genes in hyaloid vessels from WT and CLEC14A KO mice. n = 3 per group. (**I**-**K**) Relative GAPDH-normalised mRNA levels of VEGFR-3, CLEC14A and VEGFR-2 after silencing of VEGFR-3. (**L**) Immunostaining for CLEC14A, VEGFR-3 and CD31 in retinas from WT mice at P5 demonstrating co-localisation of CLEC14A and VEGFR-3. n = 3 per group. All experiments were repeated on at least 4 different sets of WT and KO littermates. *, $P < 0.05$; **, $P < 0.005$; ***, $P < 0.0001$ by paired, 2-tailed Student's *t* test. Error bars represent the mean $\pm$ SD.

Supplemental Figure 7

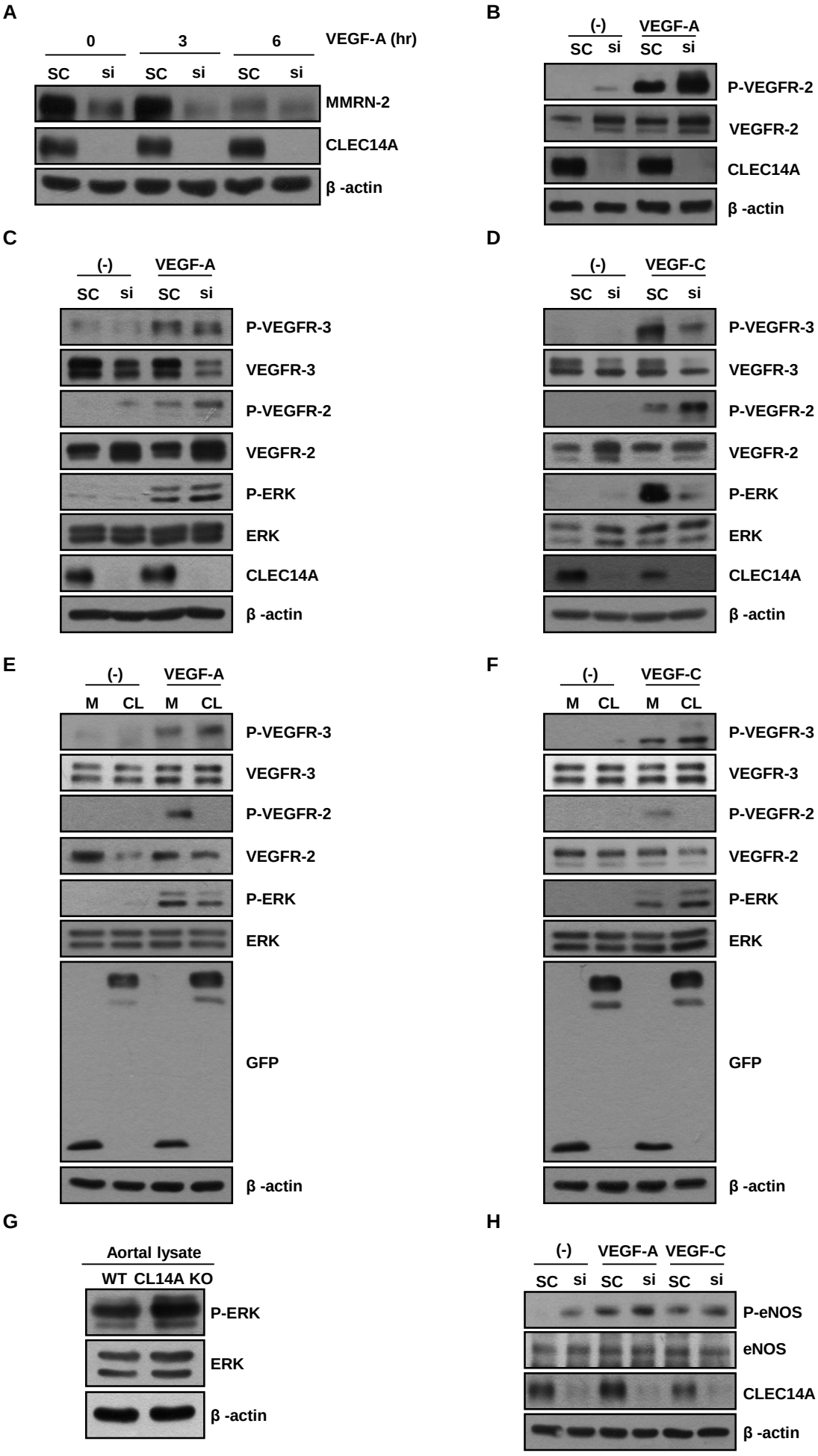

Supplemental Figure 7

CLEC14A deficiency results in decreased MMRN-2 and increased VEGFR-2 along with its downstream signalling while overexpression of CLEC14A reverses VEGFR-3 and VEGFR-2 signalling.

(**A**) Time-dependent decreases in MMRN-2 expression following silencing of CLEC14A and treatment with VEGF-A (50 ng/mL) (**B**) Increased VEGFR-2 phosphorylation and VEGFR-2 expression in HUVEC lysates after CLEC14A silencing using siRNA (50nM) and 50 ng/mL VEGF-A treatment. (**C**) Decreased phosphoactivation and expression of VEGFR-3 and increased phosphoactivation and expression of VEGFR-2 following increase in the phosphoactivation of ERK in HDLECs after knockdown of CLEC14A using siRNA (50 nM) and stimulation with 50 ng/mL VEGF-A for 5 min (**D**) Decreased phosphoactivation and expression of VEGFR-3 following decrease in the phosphoactivation of ERK and increased phosphoactivation and expression of VEGFR-2 in HDLECs after knockdown of CLEC14A using siRNA (50 nM) and treatment with 100 ng/mL VEGF-C for 15 min (**E**) Elevated phosphoactivation and expression of VEGFR-3 and reduced phosphoactivation and expression of VEGFR-2 following decrease in phosphoactivation of ERK in HDLECs after overexpression of GFP-tagged CLEC14A together with VEGF-A (50 ng/mL) for 5 min (GFP-Mock and GFP-CLEC14A-FL). (**F**) Enhanced phosphoactivation and expression of VEGFR-3 following increase in phosphoactivation of ERK and decreased phosphoactivation and expression of VEGFR-2 after overexpression of GFP-tagged CLEC14A together with VEGF-C (100 ng/mL) treatment for 15 min in HDLECs (GFP-Mock and GFP-CLEC14A-FL). (**G**) Increased ERK phosphorylation in P6 CLEC14A KO aorta lysate. n = 3 per group. (**E**) Increased eNOS phosphorylation upon silencing of CLEC14A with the treatment of VEGF-A or –C (VEGF-A: 50 ng/mL, VEGF-C: 100 ng/mL). All experiments were repeated at least 3 different sets.

Supplemental Figure 8

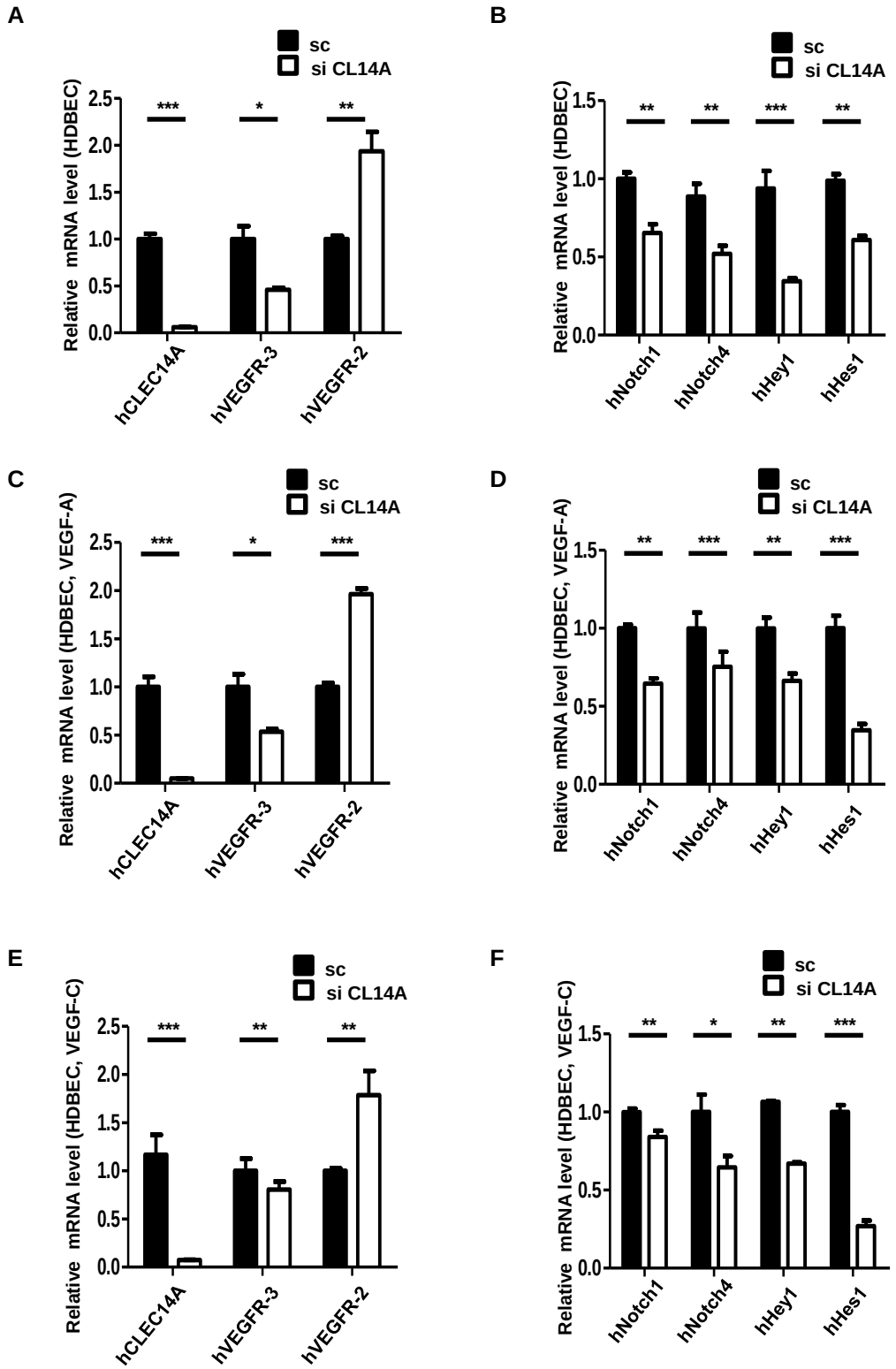

Supplemental Figure 8

Upon VEGF-A and VEGF-C treatment, silencing of CLEC14A changes the expression levels of VEGFR-3, VEGFR-2, Notch and Notch target genes in HDBECs

(**A** and **B**) Relative GAPDH-normalised mRNA levels of CLEC14A, VEGFR-3 and VEGFR-2, Notch and Notch target genes after CLEC14A silencing in HDBECs. (**C** and **D**) Relative GAPDH-normalised mRNA levels of CLEC14A, VEGFR-3, VEGFR-2, Notch and Notch target genes in HDBECs following treatment of VEGF-A (50 ng/mL) (**E** and **F**) Relative GAPDH-normalised mRNA levels of CLEC14A, VEGFR-3, VEGFR-2, Notch and Notch target genes in HDBECs following treatment of VEGF-C (100 ng/mL). *, $P < 0.05$; **, $P < 0.005$; ***, $P < 0.0001$ by paired, 2-tailed Student's *t* test. All experiments were repeated at least 3 different sets. Error bars represent the mean $\pm$ SD.

Supplemental Figure 9

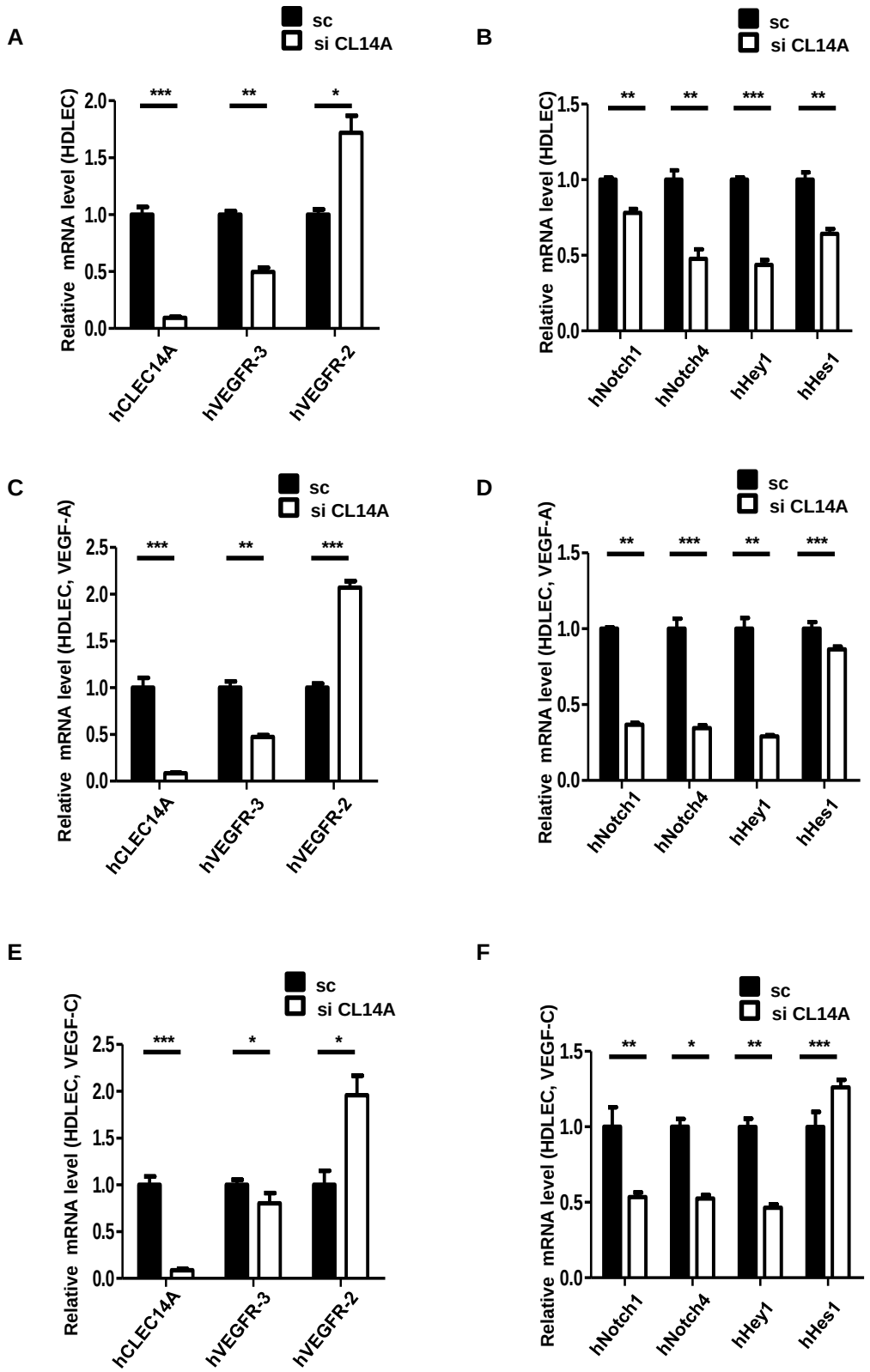

Supplemental Figure 9

Upon VEGF-A and VEGF-C treatment, silencing of CLEC14A changes the expression levels of VEGFR-3, VEGFR-2, Notch and Notch target genes in HDLECs

(**A** and **B**) Relative GAPDH-normalised mRNA levels of CLEC14A, VEGFR-3 and VEGFR-2, Notch and Notch target genes after CLEC14A silencing in HDLECs. (**C** and **D**) Relative GAPDH-normalised mRNA levels of CLEC14A, VEGFR-3, VEGFR-2, Notch and Notch target genes in HDLECs following treatment of VEGF-A (50 ng/mL) (**E** and **F**) Relative GAPDH-normalised mRNA levels of CLEC14A, VEGFR-3, VEGFR-2, Notch and Notch target genes in HDLECs following treatment of VEGF-C (100 ng/mL). *, $P < 0.05$; **, $P < 0.005$; ***, $P < 0.0001$ by paired, 2-tailed Student's *t* test. All experiments were repeated at least 3 different sets. Error bars represent the mean $\pm$ SD.

Supplemental Figure 10

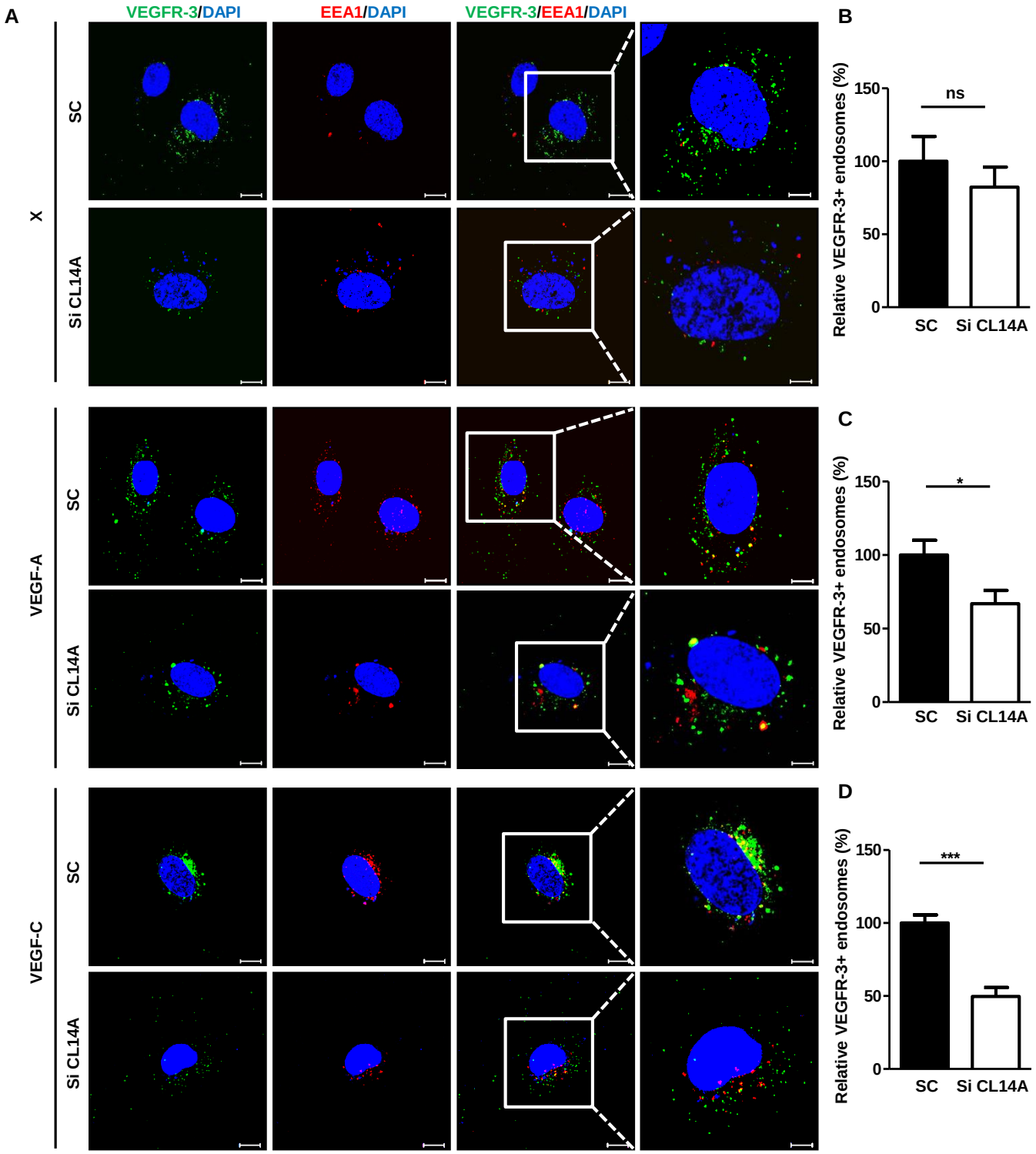

Supplemental Figure 10

Knockdown of CLEC14A reduces the internalization of VEGFR-3 after exposure to VEGF-C in HDBECs

(**A**) Immunocytochemical staining of VEGFR-3 and EEA1 in untreated, VEGF-A-treated (50 ng/mL), and VEGF-C-treated cells (100 ng/mL) demonstrating reduced internalization of VEGFR-3 after VEGF-C treatment. Scale bar: 10 μm and 5 μm for enlarged images. (**B**-**D**) Quantification of the percent internalization of VEGFR-3 after exposure to no ligand, VEGF-A-, or VEGF-C-. All experiments were repeated at least 3 different sets. *, $P < 0.05$; **, $P < 0.005$; ***, $P < 0.0001$ by paired, 2-tailed Student's *t* test. Error bars represent the mean $\pm$ SD.

Supplemental Figure 11

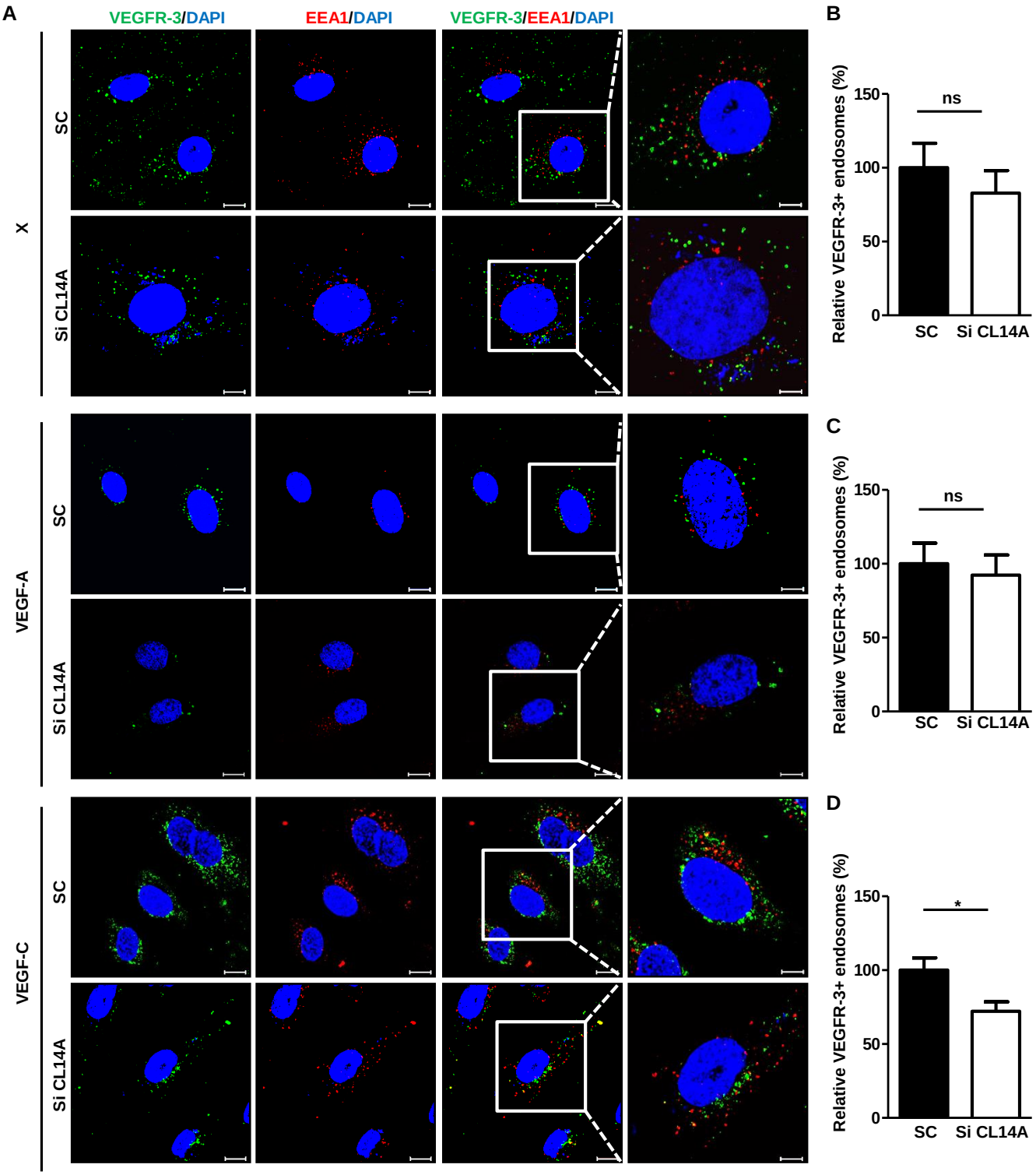

Supplemental Figure 11

Knockdown of CLEC14A reduces the internalization of VEGFR-3 after exposure to VEGF-C in HDLECs

(**A**) Immunocytochemical staining of VEGFR-3 and EEA1 in untreated, VEGF-A-treated (50 ng/mL), and VEGF-C-treated cells (100 ng/mL) demonstrating reduced internalization of VEGFR-3 after VEGF-C treatment. Scale bar: 10 μm and 5 μm for enlarged images. (**B**-**D**) Quantification of the percent internalization of VEGFR-3 after exposure to no ligand, VEGF-A-, or VEGF-C-. All experiments were repeated at least 3 different sets. *, $P < 0.05$; **, $P < 0.005$; ***, $P < 0.0001$ by paired, 2-tailed Student's *t* test. Error bars represent the mean $\pm$ SD.

Supplemental Figure 12

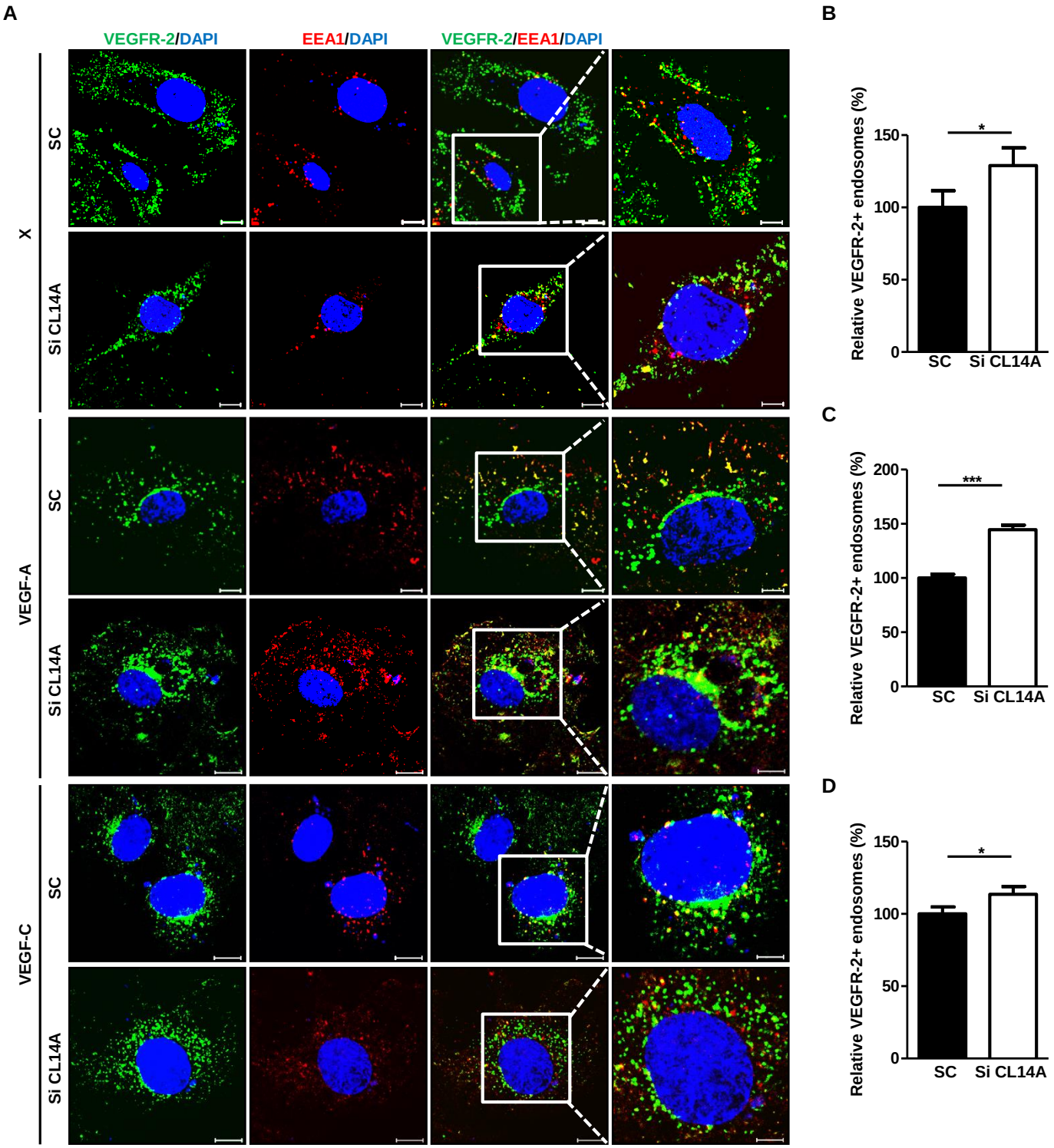

Supplemental Figure 12

Knockdown of CLEC14A enhances the internalization of VEGFR-2 after exposure to VEGF-A in HDBECs

(**A**) Immunocytochemical staining of VEGFR-2 and EEA1 in untreated, VEGF-A-treated (50 ng/mL), and VEGF-C-treated cells (100 ng/mL) demonstrating reduced internalization of VEGFR-2 after VEGF-A treatment. Scale bar: 10 μm and 5 μm for enlarged images. (**B**-**D**) Quantification of the percent internalization of VEGFR-2 after exposure to no ligand, VEGF-A-, or VEGF-C-. All experiments were repeated at least 3 different sets. *, $P < 0.05$; **, $P < 0.005$; ***, $P < 0.0001$ by paired, 2-tailed Student's *t* test. Error bars represent the mean $\pm$ SD.

Supplemental Figure 13

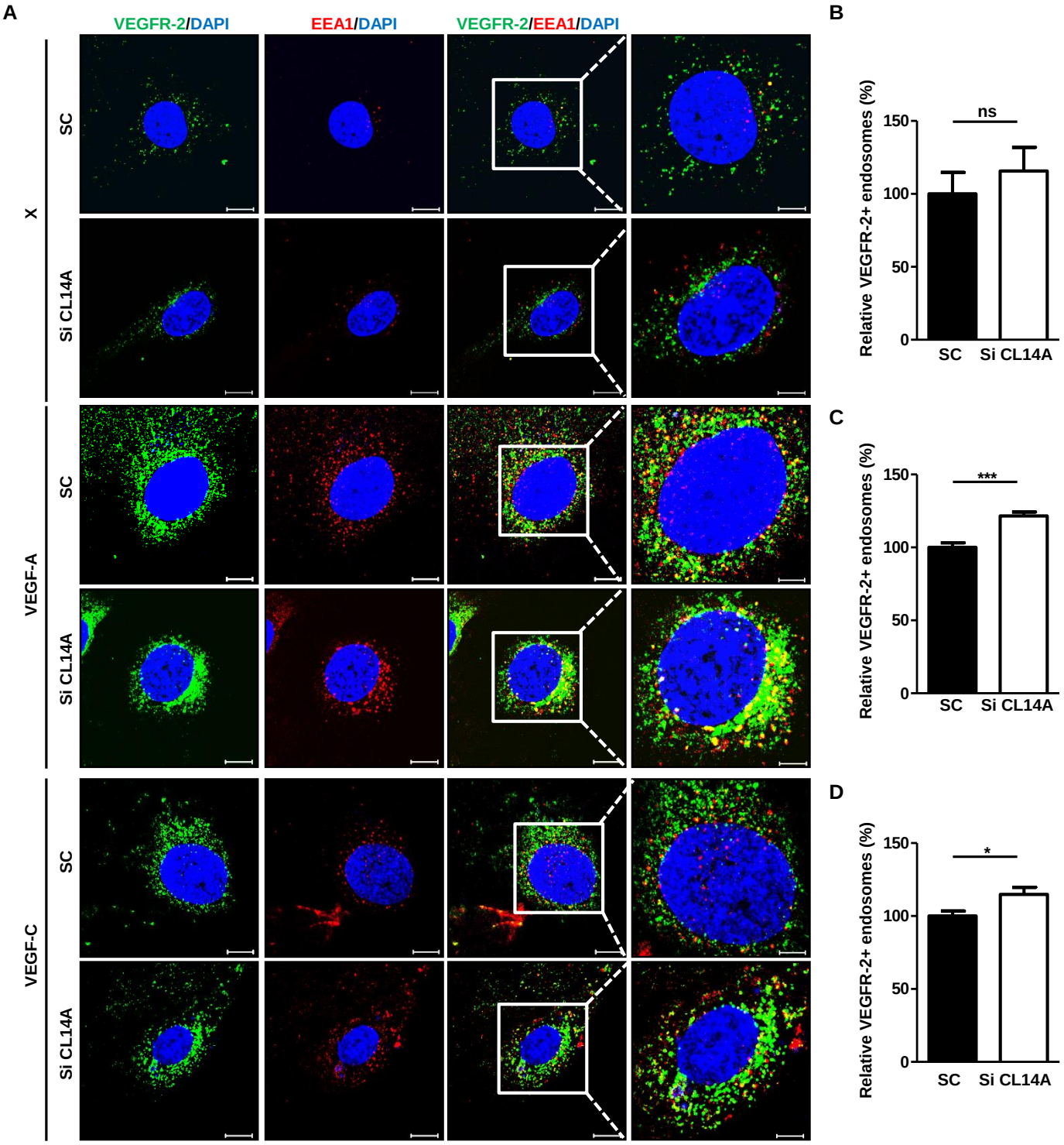

Supplemental Figure 13

Knockdown of CLEC14A enhances the internalization of VEGFR-2 after exposure to VEGF-A in HDLECs

(**A**) Immunocytochemical staining of VEGFR-2 and EEA1 in untreated, VEGF-A-treated (50 ng/mL), and VEGF-C-treated cells (100 ng/mL) demonstrating reduced internalization of VEGFR-2 after VEGF-A treatment. Scale bar: 10 μm and 5 μm for enlarged images. (**B**-**D**) Quantification of the percent internalization of VEGFR-2 after exposure to no ligand, VEGF-A-, or VEGF-C-. All experiments were repeated at least 3 different sets. *, $P < 0.05$; **, $P < 0.005$; ***, $P < 0.0001$ by paired, 2-tailed Student's *t* test. Error bars represent the mean $\pm$ SD.

Supplemental Figure 14

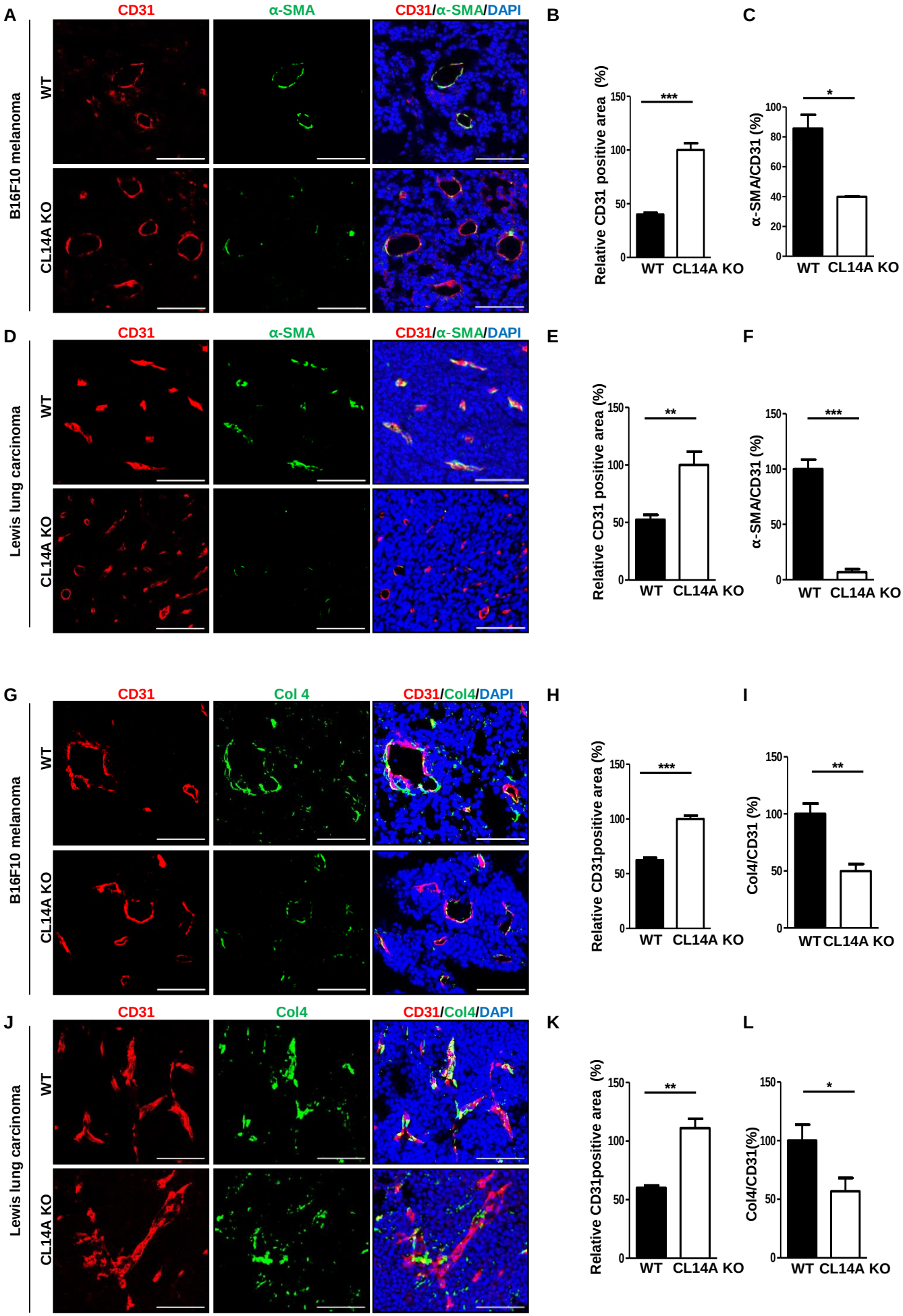

Supplemental Figure 14

CLEC14A deficiency leads to increased tumor angiogenesis and vascular abnormalities

(**A**) CD31 and α-SMA staining of B16F10 tumors grown in WT and CLEC14A KO mice. n = 6 per group. (**B** and **C**) Quantification of the CD31-positive area and the α-SMA:CD31 ratio (%). (**D**) CD31 and α-SMA staining of LLC tumors grown in WT and CLEC14A KO mice. n = 6 per group. (**E** and **F**) Quantification of the CD31-positive area and α-SMA:CD31 ratio. (**G**) CD31 and collagen type IV (Col4) staining of B16F10 tumors grown in WT and CLEC14A KO mice. n = 6 per group. (**H** and **I**) Quantification of the CD31-positive area and Col4:CD31 ratio. (**J**) CD31 and Col4 staining of LLC tumors grown in WT and CLEC14A KO mice. n = 6 per group. (**K** and **L**) Quantification of the CD31-positive area and Col4:CD31 ratio. Scale bar: 100 μm. n = 6 per group. *, $P < 0.05$; **, $P < 0.005$; ***, $P < 0.0001$ by paired, 2-tailed Student's *t* test. Error bars represent the mean ± SD.

Supplemental Figure 15

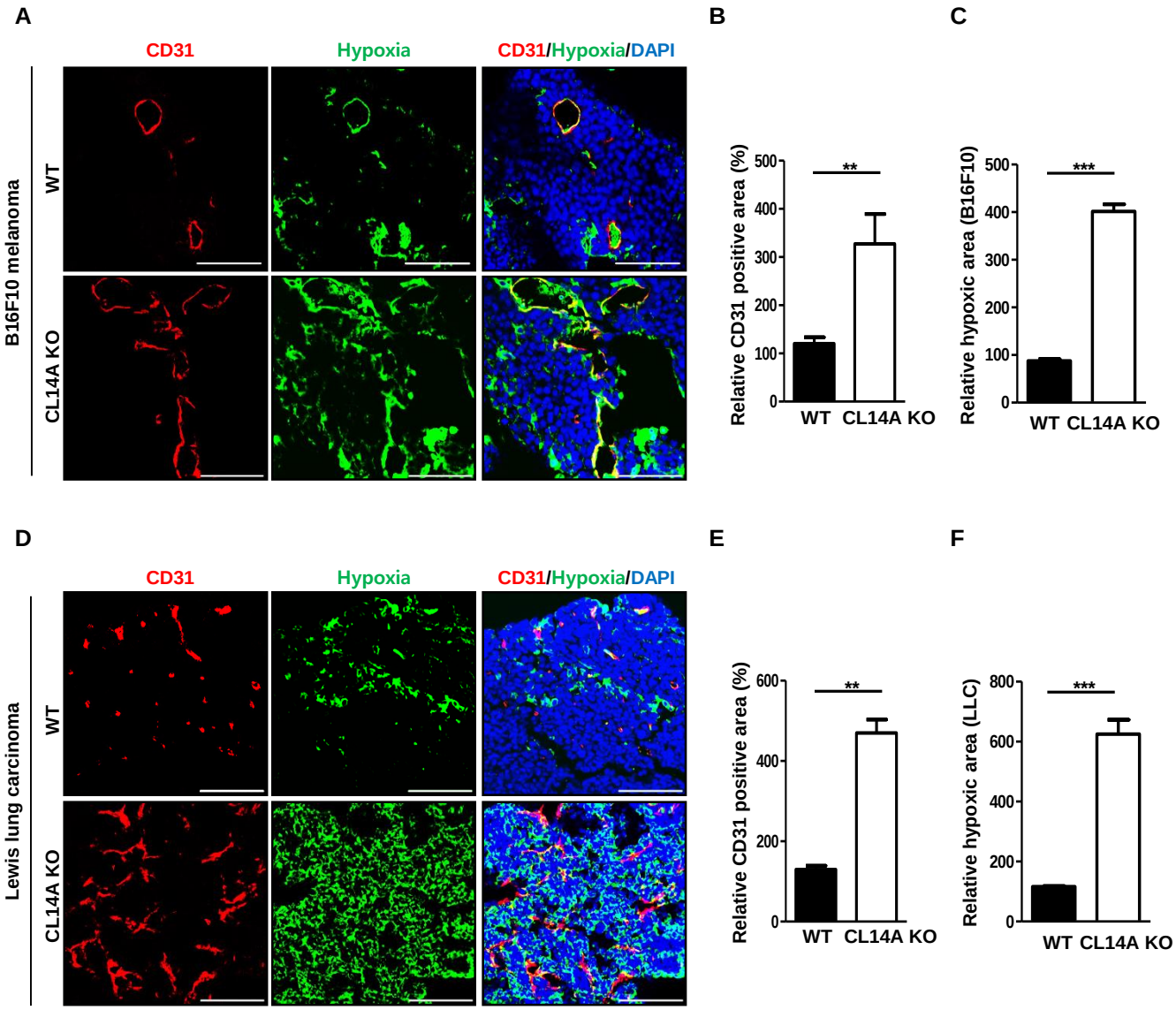

Supplemental Figure 15

Elevated hypoxia in B16F10 and LLC of CLEC14A KO mice

(**A**) CD31 and hypoxyprobe staining of B16F10 tumors grown in WT and CLEC14A KO mice. n = 6 per group. (**B** and **C**) Quantification of the CD31-positive area and relative hypoxic area (%). (**D**) CD31 and hypoxyprobe staining of LLC tumors grown in WT and CLEC14A KO mice. n = 6 per group. (**E** and **F**) Quantification of the CD31-positive area and relative hypoxic area (%). Scale bar: 100 μm. *, $P < 0.05$; **, $P < 0.005$; ***, $P < 0.0001$ by paired, 2-tailed Student's *t* test. Error bars represent the mean $\pm$ SD.

Supplemental Figure 16

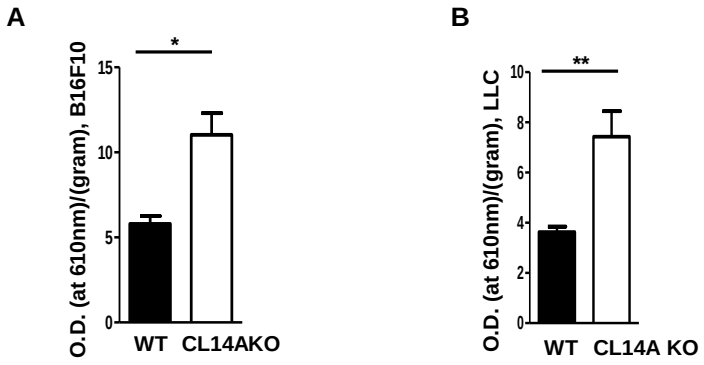

Supplemental Figure 16

Increased extravasation of the dye in tumors grown in CLEC14A KO mice

(**A**) Quantification of extravasated Evans blue in B16F10 tumors (O.D. at 610 nm per gram of tissue). (**B**) Quantification of extravasated Evans blue in LLC tumors (O.D. at 610 nm per gram of tissue). n = 6 per group. *, $P < 0.05$; **, $P < 0.005$; ***, $P < 0.0001$ by paired, 2-tailed Student's *t* test. Error bars represent the mean $\pm$ SD.

Supplemental Figure 17

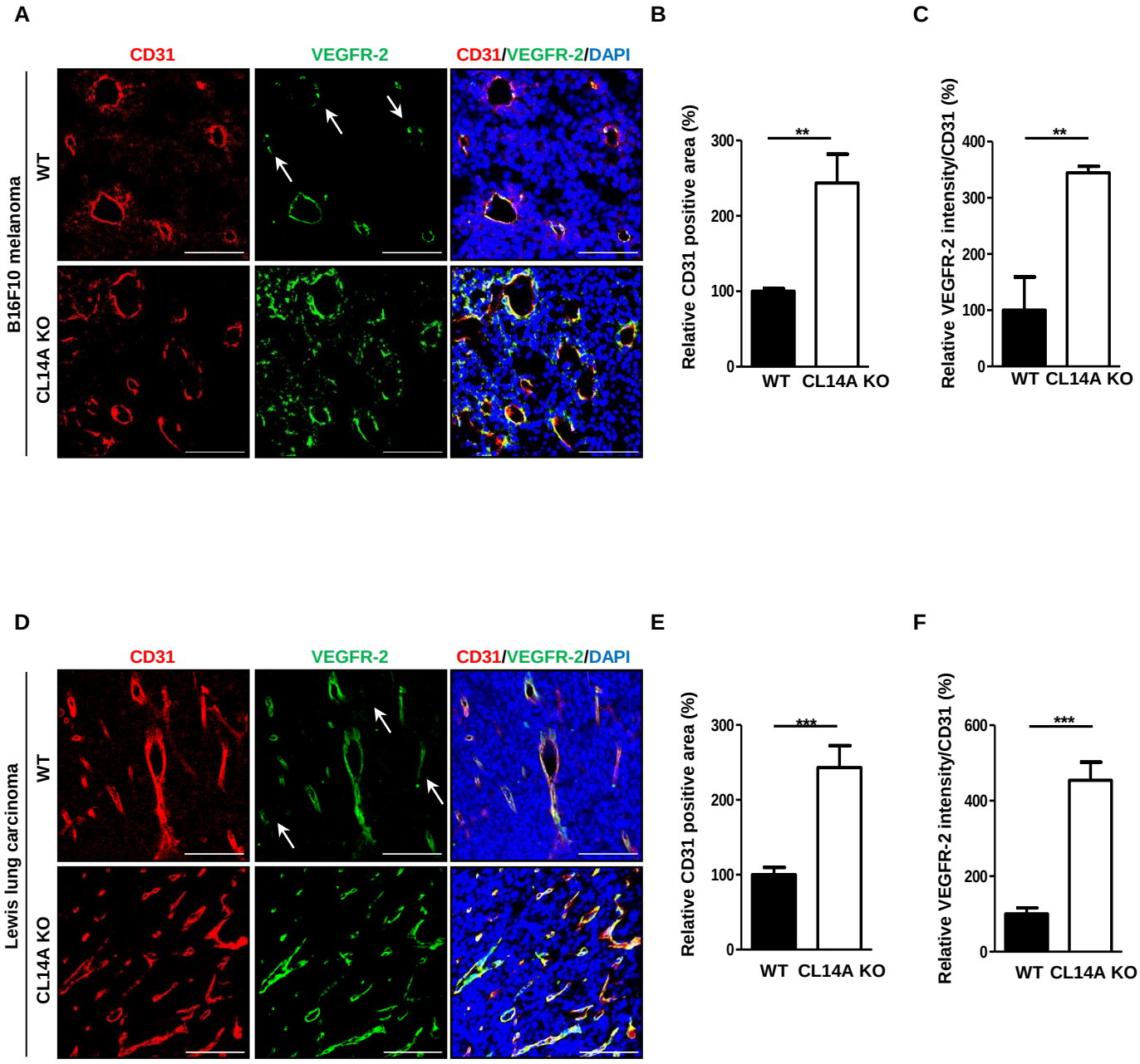

Supplemental Figure 17

CLEC14A deficiency increased VEGFR-2 expression in B16F10 and LLC tumors

(**A**) Immunostaining for CD31 and VEGFR-2 in B16F10 tumors grown in WT and CLEC14A KO mice. n = 6 per group. (**B** and **C**) Quantification of the CD31-positive area and relative VEGFR-2 intensity (normalised to CD31 intensity) in B16F10 tumors (% of control). (**D**) CD31 and VEGFR-2 immunostaining of LLC tumors grown in WT and CLEC14A KO mice. n = 6 per group. (**E** and **F**) Quantification of CD31 and relative VEGFR-2 intensity (normalised to CD31 intensity) in LLC tumors (% of control). White arrows indicate weak expression of VEGFR-2. Scale bar: 100 μm. *, $P < 0.05$; **, $P < 0.005$; ***, $P < 0.0001$ by paired, 2-tailed Student's *t* test. Error bars represent the mean $\pm$ SD.

Supplemental Figure 18

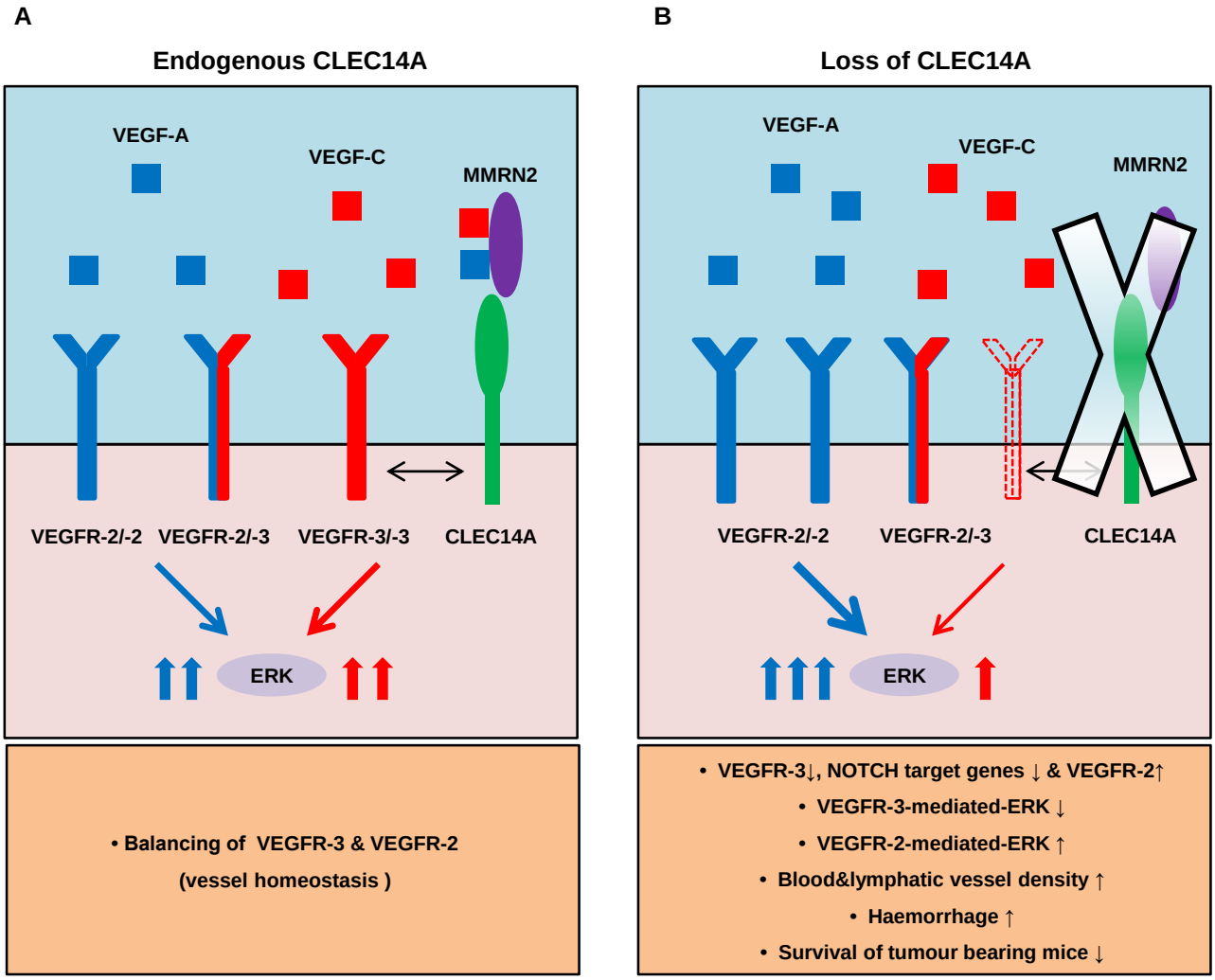

Supplemental Figure 18

Schematic diagram: the role of CLEC14A

(**A**) CLEC14A balances VEGFR-3 and VEGFR-2 signaling and expression, modulating blood and lymphatic vessel homeostasis. (**B**) CLEC14A deletion results in reduced VEGFR-3 and increased VEGFR-2 phosphorylation and expression, showing abnormal blood and lymphatic vasculature during development and in pathological conditions.

Supplemental Table 1 Primer sequences used for genotyping confirmation

Gene	Sequence
mCLEC14A-neo-fwd	5`-TCATTCTCAGTATTGTTTTG-3`
mCLEC14A-rev-SD	5`-GAATAGGAAAATGTCTCTTG-3`
mCLEC14A-intra-fwd	5`-GAGCATAGCAGTTATCGTTT-3

Supplemental Table 2 Primer sequences used for Q-PCR analysis of WT and CLEC14A KO mice

Gene	Sequence
mCLEC14A-5'UTR-fwd	5`-TTCCTTTTCCAGGGTTTGTG;-3`
mCLEC14A-5'UTR-rev	5`-GCCTACAAGGTGGCTTGAAT-3`
mCLEC14A-CDS-fwd	5′-AAGCTGTGCTCCTGCTCTTG-3′
mCLEC14A-CDS-rev	5′-TCCTGAGTGCACTGTGAGATG-3′
mCLEC14A-3'UTR-fwd	5′-CTGTAGAGGGCGGTGACTTT-3′
mCLEC14A-3'UTR-rev	5`-AGCTGCTCCCAAGTCCTCT-3

Supplemental Table 3 Primer sequences used for real time PCR

Gene	Forward (5`->3`)	Reverse (5`->3`)
hGAPDH	CGCCACAGTTTCCCGGAGGG	CCCTCCAAAATCAAGTGGGG
hCLEC14A	CTGGGACCGAGGTGA	CGCGATGCAAGTAACTGAGA
hVEGFR-2	CTACCTCACCTGTTTCCTGTATG	GTCCGTCTGGTTGTCATCTG
hVEGFR-3	CCACACAGAACTCTCCAGCA	ACAATGACCTCGGTGCTCTC
hDll4	TGGGTCAGAACTGGTTATTGGA	GTCATTGCGCTTCTTGCACAG
hNotch1	CACTGTGGGCGGGTCC	GTTGTATTGGTTCGGCACCAT
hHey1	GAGAAGCAGGGATCTGCTAA	CCCAAACTCCGATAGTCCAT
hHes1	CGGACATTCTGGAAATGA CA	CATTGATCTGGGTCATGCAG
hNrarp	TGAAGCTGCTGGTCAAGTTC	TAGTTGGCGGGAAGGTACAG
hFoxC2	GCAACCCAACAGCAAACTTTC	GACGGCGTAGCTCGATAGG
mGAPDH	CAACGACCCCTTCATTGACC	AGTGATGGCATGGACTGTGG
mCLEC14A	GACCAAAGTTGAAGAACAGC	GAAGAGGTGTCGAAAGTCAG
mVEGFR-2	CTACCCCAGAAATGTACCAGAC	AATCCTCTTCCATGCTCAGTG
mVEGFR-3	TGGCAAATGGTTACTCCATGACCC	ACATCGAGTCCTTCCTGTTGACCA
mDll4	GGAACCTTCTCACTCAACATCC	CTCGTCTGTTCGCCAAATCT
mNotch1	GCAGTTGTGCTCCTGAAGAA	CGGGCGGCCAGAAAC
mHey1	CATGAAGAGAGCTCACCCAGA	CGCCGAACTCAAGTTTCC
mHes1	ACACCGGACAAACCAAAGAC	CGCCTCTTCTCCATGATAGG
mNrarp	TGCTGCAGAACATGACTAAC	GCCTTGGTGATGAGATAGAG
mFoxC2	CCTTCTACCGCGAGAACAAG	CCGGGTCGAGCGTCCAGTAG